Sixth International Symposium on Turbulence and Shear Flow Phenomena
Seoul, Korea, 22-24 June 2009

LES OF FLOW PAST CIRCULAR AND ELLIPTIC CYLINDERS IN PROXIMITY TO A WALL

Subrata Sarkar
Department of Mechanical Engineering,
Indian Institute of Technology Kanpur
Kanpur- 208016, UP, India
subra@iitk.ac.in

Sudipto Sarkar
Department of Mechanical Engineering,
Indian Institute of Technology Kanpur
Kanpur- 208016, UP, India
sudipto@iitk.ac.in

ABSTRACT

Flow past a circular (axis ratio, AR = 1) and elliptical cylinders of different AR (AR = 2, 3, 4) in the vicinity of a wall have been investigated for a constant gap-to-diameter ratio, G/D = 0.5 (where, G signifies the gap between the cylinder and flat plate and D the elliptic cylinder minor diameter). Large-eddy simulations (LES) have been carried out with the dynamic subgrid model for a Reynolds number, Re = 1440 (based on D and free-stream velocity U_∞). Simulations have also been performed for three different G/D ratios of 0.25, 0.5 and 1.0 following the experiment of Price et al. [2002], where a circular cylinder was used. The unsteady, three-dimensional Navier-Stokes equations have been solved on a staggered mesh arrangement using a symmetry-preserving central difference scheme, which is widely used in LES owing to its non-dissipative and conservative property. The immersed boundary (IB) method is employed to impose the no-slip boundary condition on the cylinder surface. An attempt is made to understand the physics of flow involving interactions of shear layers shed from the cylinder and the wall boundary layer. Present LES reveals the shear layer instability and formation of small-scale eddies apart from their mutual interactions with the boundary layer. It has been observed that both the shape of the cylinder and the G/D ratio have a strong influence on the modification of wake dynamics and evolution of the wall boundary layer.

1. INTRODUCTION

Since the beginning of the manned flight, the pilots have experienced an upward force on the aircraft at the time of landing. This can be attributed to the air trapped between the wings and the runway forming an air cushion, which is known as ground effect in aerodynamic term. Most of the past studies made so far to understand the flow physics related to the ground effect have considered the body as a circular cylinder [Taneda 1965; Bearman and Zdravkovich, 1978; Grass et al., 1984; Taniguchi and Miyakoshi, 1990; Lei et al., 1999; Price et al., 2002]. The major modifications in the flow dynamics of flow past a cylinder in the vicinity of a wall can be identified as: (1) deflection of the boundary layer away from the flat plate, (2) suppression of vortex shedding from the lower half of the cylinder, (3) presence of separation bubble both upstream and downstream of the cylinder and (4) a significant change of flow parameters such as lift, drag coefficients and Strouhal number.

In most of the experiments for flow around a circular cylinder in the presence of the boundary layer, the approaching boundary layer was turbulent [Bearman and Zdravkovich, 1978; Grass et al., 1984; Taniguchi and Miyakoshi, 1990 and Lei et al., 1999]. Here, the aerodynamic forces on the cylinder were modified with a slight variation of shedding frequency. The suppression of vortex shedding was observed when the body was closer than a critical distance from the wall such that G/D ratio becomes 0.3-0.4 [Bearman and Zdravkovich, 1978]. At smaller distances, the wake is almost steady and the periodic shedding is strongly inhibited with separation bubbles on the wall. Later, Lei et al. [1999] reported that the suppression of vortex shedding occurs at a gap ratio of about 0.2-0.3. This critical gap ratio decreases as the thickness of the boundary layer increases.

The flow visualization around a circular cylinder near a wall was demonstrated by Price et al. [2002] for Re in the range of shear layer transition region (Re = 1200 – 4960) and G/D in between 0-2. They concluded that G/D was a major factor for the change of flow characteristics. The flow interactions between the cylinder wake and the boundary layer were divided in four regimes based on G/D ratio. The paper presented the flow structures and modification of wake dynamics with the help of instantaneous flow field and Strouhal frequency (St) They observed that for Re < 2600, St for G/D < 2 was significantly greater than that of an isolated cylinder. But as Re increased (Re > 4000), St became insensitive to the G/D ratio. However, the paper lacked the discussion on aerodynamic forces, mean velocity field and turbulence characteristics.

As compared to the experiments, there are a few numerical simulations of flow past a circular cylinder in the vicinity of flat plate. Vada et al. [1989] were the first to perform a 2-D simulation using vortex in cell method at a

transcritical Reynolds number, $Re = 3.6 \times 10^6$ and G/D = 0.4, 0.8 and 1.5. The simulation suffered from over prediction of drag coefficient and under prediction of lift coefficient as compared to the experiment [Zdravkovich, 1985]. Liou et al. [2002] performed a LES of the turbulent wake behind a square cylinder for a $Re = 2.2 \times 10^4$ and the discussion were focused on the phase-averaged vortex dynamics. The celerity of the positive vortex shed from the lower side of the cylinder was smaller than that of the upper side shed vortex due to the interaction with the boundary layer. Recently Dipankar and Sengupta [2005] performed a 2-D simulation of cylinder-boundary layer interaction with ψ-ω formulation at Re = 1200 and for G/D = 0.5 and 1.5. The computation illustrated larger vortical structures as compared to the experiment of Price et al. [2002] with rollup of vortices closer to the cylinder. This was attributed to the fact that the absence of spanwise direction in 2-D simulation failed to redistribute the energy in the third direction developing unrealistic large structures [Mittal and Balachandar, 1995].

Studies of flow characteristics past an elliptic cylinder in the presence of a wall are very limited, although elliptic cylinders have the general fluid dynamic features between those of a circular cylinder and a flat plate. Moreover, elliptic cross-sectional cylinder is a better replacement of an aircraft. Choi and Lee [2000, 2001] carried out experiments on elliptic cylinders (AR = 2) near a wall for varying G/D ratio and angle of attack. The cylinder was embedded in a turbulent boundary layer ($Re = 1.4 \times 10^4$) whose thickness was larger than the cylinder height. When compared with a circular cylinder under the same conditions, they observed smaller variation of pressure distributions on the surface, faster recovery of pressure on the flat plate and a relatively small wake region behind the elliptic cylinder. The suppression of vortex shedding occurred at a relatively high G/D ratio as compared to a circular cylinder. For an inclined elliptic cylinder, Choi and Lee [2001] observed differences in vortex-shedding frequency with varying angles of attack. Also, the boundary layer near the wall was disturbed more for a negative angle of attack than that of a positive angle of attack. As per the authors knowledge, no computational work has been published on ground effect of an elliptic cylinder.

The objective of the present paper is to characterize the vortex shedding illustrating the flow physics in terms of vortex stretching, breakdown and turbulence generation as G/D and AR of the cylinder changes. Here, we try to explain the mutual interactions, i.e., modification of wake dynamics due to the presence of the boundary layer and the excitation of boundary layer because of the wake. It should be noted that the eddy motions and their interactions are expected to be resolved to understand the dynamical process in turbulent flows for the concerned problem. A direct numerical simulation (DNS) would have been ideal for the problem, but it is extremely costly and Reynolds-averaged Navier-Stokes calculations will not provide the answer. Hence, LES can be pursued as an alternative means with the benefit being a considerably lower computational effort. In the present study, a 3-D LES with a dynamic subgrid-scale model has been used to investigate the flow around a circular and an elliptic (AR2) cylinder in proximity of a wall boundary layer at Re = 1440 and for G/D of 0.25, 0.5 and 1.0. Also elliptic cylinders with high AR (AR3 and AR4) have been computed at the same Re for G/D = 0.5 to understand the effect of body shape on wake-boundary layer interactions.

2. Numerical Methods

2.1 Governing Equations

In the present study, we perform LES of incompressible flow. The filtered mass and momentum equations can be expressed as,

$$\frac{\partial \overline{u}_j}{\partial x_j} = 0 \qquad (1)$$

$$\frac{\partial \overline{u}_i}{\partial t} + \frac{\partial}{\partial x_j}\left(\overline{u}_j \overline{u}_i\right) = -\frac{1}{\rho}\frac{\partial \overline{P}}{\partial x_i} + \frac{1}{\mathrm{Re}}\nabla^2 \overline{u}_i - \frac{\partial \tau_{ij}}{\partial x_j} + \overline{f}_i \qquad (2)$$

where, $\overline{u_i}$ denotes the filtered velocity field and $\tau_{ij} = \overline{u_i u_j} - \overline{u}_i \overline{u}_j$ is the residual stress tensor (also known as subgrid-scale stress, SGS). The presence of the body forces $\overline{f_i}$ is due to the IB method (Fadlun et al., 2000). The velocity field near the boundary of the body is modified at each step in such a way that the no-slip boundary condition is satisfied on the surface. This is done using some interpolations, which is equivalent to include a body force $\overline{f_i}$ in the momentum equation. In this paper, a quadratic unidirectional interpolation of Muldoon and Acharya [2005] is used. The equations (1) and (2) have been made dimensionless using the inlet free-stream velocity U_∞ and the cylinder diameter D. The resulting Reynolds number is defined as $\mathrm{Re} = U_\infty D/\nu$, ν being the kinematic viscosity. The model proposed by Germano et al. [1991] and modified by Lilly [1992] is used here to include the effect of subgrid motions in the resolved LES, where the model coefficient is dynamically calculated instead of input a priori. The momentum advancement is explicit using the second-order Adams-Bashforth scheme, except for the pressure term, which is solved by a standard projection method [Chorin, 1968]. The pressure equation is discrete Fourier transformed in the spanwise direction (an infinite cylinder is assumed neglecting the end effects and hence the flow can be considered homogeneous allowing periodicity of flow to be imposed) and is solved by the BI-CG algorithm [Zhang, 1997] in the other two directions. The spatial discretization is second-order accurate on a staggered mesh arrangement using a symmetry-preserving central-difference scheme, which is widely used in LES owing to its non-dissipative and conservative property [Mittal and Moin, 1997, Morinishi et al., 1998].

Here, the simulations of flow past a cylinder in proximity to a wall have been performed in the Cartesian grid considering the origin of axes lies on the flat plate and at a distance of 10D from the leading edge. The co-ordinates x, y, z denote the streamwise, wall-normal and spanwise directions respectively and the corresponding velocities are denoted by u, v and w. The domain extends from -5D at the inflow to 25D at the outflow with a spanwise length of 3D.

In the wall-normal direction, the domain is extended up to 9*D* for *G/D* = 1.0 (both for AR1 and AR2) and 8.5*D* for all other cases. A Blasius profile is imposed at the inlet considering the computational domain begins at a 5*D* distance downstream from the leading edge of the flat plate, where the boundary layer thickness is considered as 0.295*D*. The computational domain and boundary conditions used here are illustrated in Fig. 1.

2.2 Computational Details

In the streamwise direction, a uniform and refined mesh is used near the cylinder to get adequate immersed-boundary points on the cylinder surface. In the flow-normal direction, a refined and uniform mesh is employed near the wall (up to *y/D* = 2 for *G/D* = 0.25, 0.5 and *y/D* = 2.5 for *G/D* = 1.0) to resolve the wake behind the cylinder and its interaction with the boundary layer. Away from the cylinder, the mesh is slowly stretched out.

A mesh of 384×192×32 is chosen after a grid resolution test for flow past a circular cylinder in proximity to a wall for *G/D* = 0.25. Among 384 streamwise grid points, 40 points are distributed upstream of the cylinder (-5*D* to -*D*), 96 points surrounding the cylinder (-*D* to +*D*), 160 points near wake region (+*D* to +10*D*) and rest are distributed in the far field downstream (+10*D* to +25*D*). In the wall-normal direction, a total of 128 grid points with equal spacing are used between 0 to 2*D* and remaining 64 points are slowly stretched away from the cylinder (+2*D* to +8.5*D*). A uniform mesh is used in the spanwise direction owing to the symmetry of the body.

The grid distribution remain same as before for AR1, *G/D* = 0.5; AR2, *G/D* = 0.25 and AR2, *G/D* = 0.5. As the cylinder tends to a slender body for increased AR, 408 grid points are used for AR4, whereas 384 points are used for AR3 but clustering of grid points towards the leading and trailing edges. The computational domain is extended by 0.5*D* in the wall-normal direction for *G/D* = 1 (AR1 and AR2) keeping the streamwise domain unchanged and with 224 points in the wall normal direction.

The time step was about $\Delta t = 1.125\times10^{-3}\left(D/U_\infty\right)$ in non-dimensional. This time kept the Courant number below 0.2 for the entire simulation and the viscous stability number was much less. The flow field was allowed to evolve for fifteen vortex-shedding cycles to get a dynamically steady state solution. Then the data were collected for statistics for a period of fifteen cycles that was found sufficient to ensure statistically converged results.

3. RESULTS AND DISCUSSION

The present computation illustrates the change of flow characteristics as compared to the flow past an isolated cylinder due to the presence of a wall. Flow visualization of a circular cylinder in proximity to a wall from the present LES are compared with the corresponding experiment [Price et al., 2002] in Fig. 2. For *G/D* = 0.25, the figure depicts the formation of separation bubbles both upstream and downstream of the cylinder, a strong pairing between the inner shear layer and the wall boundary layer, stretching of shear layers and their rollup and breakdown into smaller eddies. The deflection of the approaching boundary layer and the size of the downstream recirculation region reduce for *G/D* = 0.5. The numerical visualization of instantaneous flow field illustrates a close resemblance with the experimental observations in terms of vortex dynamics and flow structures.

The iso-surface of instantaneous spanwise vorticity in the case of an elliptic cylinder (AR2) for *G/D* = 1 is depicted in Fig. 3. This illustrates the internal growth mechanism of shear layers near a wall and the three-dimensional flow structures. The receptivity of the boundary layer to external disturbance is very prominent with appearance of longitudinal streaky structures. The perturbations created by the turbulent shear layer are amplified due to the separated boundary layer, and then the non-linear interactions of vortex stretching process create these streaks, which are characteristics of turbulent flow. The flow structures remain the same for a circular cylinder, although there are some changes in minute details. When the cylinder is placed close to the wall (*G/D* = 0.25 and 0.5), the shear layers are frozen for a considerable distance before breakdown. The boundary layer is deflected away from the wall producing a large separation region downstream.

Figure 4 illustrates the overall trajectory of vortex peaks along the streamwise direction for *G/D* = 0.5 considering all axis ratios (AR1-AR4). The figure reveals that vortices from the inner shear layer and the wall boundary layer travel in an almost parallel trajectory due to the coupling between them (being of oposite sign of vortices) and move in the wall-normal direction behind the cylinder. For AR1, a strong mutual interaction between the shed vortices is reflected by the cross-over of trajectories. Thus, the negative vortices shed from the upper side of the cylinder occupy the lower position, while the positive vortices shed from the inner side of the cylinder occupy the upper position in the sheet; a similar trend is reported by Zovato and Pedrizeetti [2001]. For high AR, the trajectories of shear layers do not cross each other. Further, the deflection of the boundary layer reduces continuously with increase of axis ratio. A maximum deflection of *y/D* = 1.7 is observed for AR1, whereas, a deflection of 1.42, 1.39 and 1.34 are seen for AR2, AR3 and AR4 respectively.

The frontal stagnation point moves towards the wall producing an upward lift (C_L) on the cylinder, when the cylinder is placed close to the wall: the magnitude differs for the circular and elliptic cross-sections (Fig. 5a). This increases the base pressure resulting in a low mean value of coefficient of drag, $\overline{C_D}$ (Fig. 5b). The similar trend in the variations of $\overline{C_L}$ and $\overline{C_D}$ was reported by Lei et al. [1999], although their values differe due to the difference of the approaching boundary layer, its character and thickness. Furthermore, $\overline{C_L}$ increases and $\overline{C_D}$ decreases as the body shape of the cylinder changes from a bluff body to an aerofoil shape for a constant gap ratio (refer Fig. 5c and d).

The iso-contours of time-averaged streamwise (u_m) velocity along a few selected mean streamlines are presented in Fig. 6 for both the circular and elliptical cylinders when *G/D* = 0.5 and 1.0. The figure depicts a large recirculation bubble over the plate for *G/D* = 0.5 in the downstream of both the cylinders. This separation region

can be attributed to the strong coupling between the inner shear layer and the boundary layer. The Kármán rolls formed by the outer and inner shear layer vortices become asymmetric because of the suppression of the boundary layer. For a relatively large gap-ratio (G/D = 1.0), the inner and outer shear layer appear symmetrical and they roll close to the cylinder. The mean flow field also illustrates that for AR = 2, the downstream separation region increases as compare to a circular cylinder for the same gap ratio. The shear layers rollup close to the cylinder forming relatively reduced recirculation regions, but the length of the downstream separation on the wall increases as the shape of the cylinder changes from a bluff body (AR1) to a slender body (AR4) for the same gap ratio, Fig. 7.

The mean streamwise velocity and turbulent kinetic energy (TKE) at few streamwise locations for different G/D and AR ratios are shown in Fig. 8. The velocity profiles and TKE downstream depend on the growth of shear layer over the cylinder and thus on the body shape. The generation of TKE is due to the mutual interactions of the shear layers and the boundary layer. The velocity deficit is observed far downstream even with negative values near the wall indicating larger separation bubble for an elliptic body with a low gap ratio. The TKE profiles illustrate that turbulence levels decrease as the shape changes from a bluff body towards a streamlined section. Furthermore with increase of gap ratio, the activities shift from the outer to the inner layer: the approaching boundary layer behaves more like an attached layer excited by external perturbations.

4. CONCLUSIONS

LES of flow past a circular and elliptic cylinders in proximity to a wall has been performed to understand the insight of flow physics involving the wake and boundary layer interactions for different gap ratios and body shapes. The resolved flow field elucidates the mutual effects, i.e., modification of wake dynamics due to the presence of boundary layer and excitation of the boundary layer because of the wake flow. For a relatively low gap ratio (G/D = 0.25 and 0.5), a strong pairing between the inner shear layer and the boundary layer is observed. This delays the shear layer transition and deflects the boundary layer immediately behind the cylinder with a relatively large separation. When the cylinder is away from the wall (G/D = 1.0), the vortex shedding is similar to the Kármán sheet but asymmetry in wake shape is still evident. These Kármán vortices excite the boundary layer in an alternate fashion that triggers its transition. In the case of elliptic cylinders with high axis ratios (AR3 and AR4), for a constant gap (G/D = 0.5), a less severe deflection of the boundary layer away from the wall can be seen as compared to AR1. Here, the rollup of shear layers and its breakdown occurs close to the downstream end of the elliptic cylinders. It creates a small wake region behind the elliptic cylinders and the turbulent stresses are smaller than those of the circular cylinder.The present LES is successful to describe the flow physics involving wake-boundary layer interactions for a combination of gap ratio and shape of the cylinder.

REFERENCES

Bearman, P. W., and Zdravkovich, M. M., 1978, “Flow around a circular cylinder near a plane boundary’’, *Journal of Fluid Mechancis*, Vol. 89, pp. 33-47.

Choi, J. H., and Lee, S. J., 2000, “Ground effect of flow around an elliptic cylinder in a turbulent boundary layer’’, *Journal of Fluids and Structures,* Vol. 14, pp. 697-709.

Choi, J. H., and Lee, S. J., 2001, “Flow characteristics around an inclined elliptic cylinder in a turbulent boundary layer’’, *Journal of Fluids and Structures*, Vol. 15, pp. 1125-1135.

Chorin, A. J., 1968, “Numerical solution of the Navier–Stokes equations’’, Mathematics of Computations, Vol. 22, pp. 745–762.

Dipankar, A., and Sengupta, T. K., 2005, “Flow past a circular cylinder in the vicinity of a plane wall’’, *Journal of Fluids and Structures*, Vol. 20, pp. 403-423

Fadlun, E. A., Verzicco, R., Orlandi, P., and Mohd-Yusof, J., 2000, “Combined immersed boundary finite difference methods for three dimensional complex flow simulations’’, *Journal of Comput Phys*, Vol. 161, pp. 35-60.

Germano, M., Piomelli, U., Moin, P., and Cabot, W. H., 1991, “A dynamic subgrid-scale eddy viscosity model’’, *Physics of Fluids A*, Vol. 3, pp. 1760-1765.

Grass, A. J., Raven, P. W. J., Stuart, R. J., and Bray, J. A., 1984, “The influence of boundary layer velocity gradients and bed proximity on vortex shedding from free spanning pipelines’’, *Journal of Energy Resources Technology*, Vol. 106, pp. 70-78.

Lei C., Cheng L. and Kavanagh K., 1999, “Re-examination of the effect of a plane boundary on force and vortex shedding of a circular cylinder’’, *Journal of wind Engineering and Industrial Aerodynamics*, Vol. 80, pp. 263-286.

Lilly, D. K., 1992, “A proposed modification of the Germano subgrid-scale closure method’’, *Physics of Fluids A*, Vol. 4, pp. 633-635

Liou, T. M., Chen, S. H., and Hwang, P. W., 2002, “Large eddy simulation of turbulent wake behind a square cylinder with a nearby wall’’, *ASME Journal of Fluid Engineering*, Vol. 124, pp. 81-90.

Mittal, R., and Balachandar, S., 1995, “Effect of three-dimensionality on the lift and drag of nominally two-dimensional cylinders’’, *Physics of Fluids* B, Vol. 7, pp. 1841-1865.

Mittal, R., and Moin, P., 1997, “Suitability of upwind-biased finite-difference schemes for large-eddy simulation of turbulent flows’’, *AIAA Journal*, Vol. 35, pp. 1415-1417.

Morinishi, Y., Lund, T. S., Vasilyev, O. V., and Moin, P., 1998, “Fully conservative higher order finite difference schemes for incompressible flow’’, *Journal of Computational Physics*, Vol. 143, pp. 90-124.

Muldoon F., and Acharya, S., 2005, “Mass conservation in immersed boundary method’’, *Proceedings of FEDSM 2005*, pp. 1-9.

Price, S. J., Sumner, D., Smith, J. G., Leong, K., and Paidoussis, M. P., 2002, “Flow visualization around a circular cylinder near to a plane wall’’, *Journal of Fluids and Structure*s, Vol. 16, pp. 175-191.

Taneda, S., 1965, “Experimental investigation of vortex streets, *Journal of Physics Society Japan*’’, Vol. 20, pp. 1714-1721.

Taniguchi, S., and Miyakoshi, K., 1990, "Fluctuating fluid forces acting on a circular cylinder and interference with a plane wall'', *Experiments in Fluids*, Vol. 9, pp. 197-204.

Vada, T., Nestegard, A., and Skomedal, N., 1989, "Simulation of viscous flow around a circular cylinder in the boundary layer near a wall'', *Journal of Fluids and Structures*, Vol. 3, pp. 579-594.

Zdravkovich, M. M., 1985, "Forces on a circular cylinder near a plane wall'', *Applied Ocean Research*, Vol. 7, pp. 197-201.

Zhang, S. L., 1997, GPBI-CG: Generalized product-type methods based on Bi-Cg for solving nonsymmetric linear systems, *SIAM Journal of Scintific Computing*, Vol. 18, pp. 537-551.

Zovatto, L., and Pedrizzetti, G., 2001,"Flow about a circular cylinder between parallel walls'', *Journal of Fluid Mechanics*,Vol.440,pp.1-25.

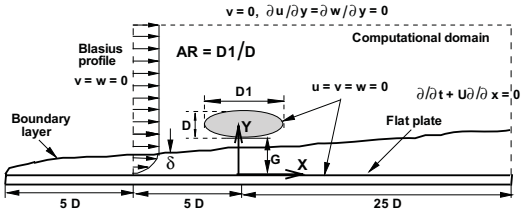

Figure 1: Computational domain with boundary conditions.

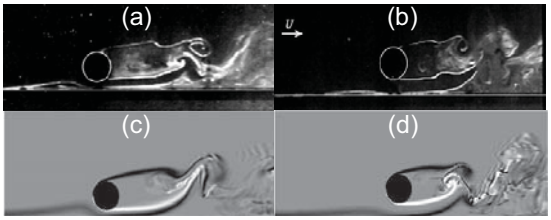

Figure 2: Instantaneous spanwise vorticity contours: (a) and (b) experiment [1]; (c) and (d) present LES; (a) and (c) G/D =0.25, (b) and (d) G/D =0.5.

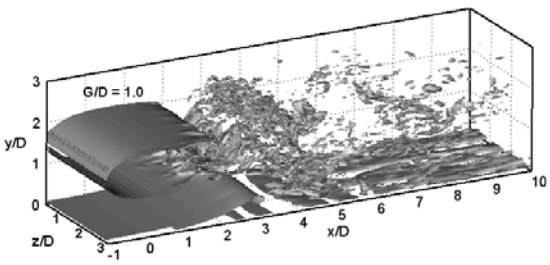

Figure 3: Iso-surfaces of instantaneous spanwise vorticity ($\omega_z = \pm 2.5$) for AR 2 and G/D = 1.0.

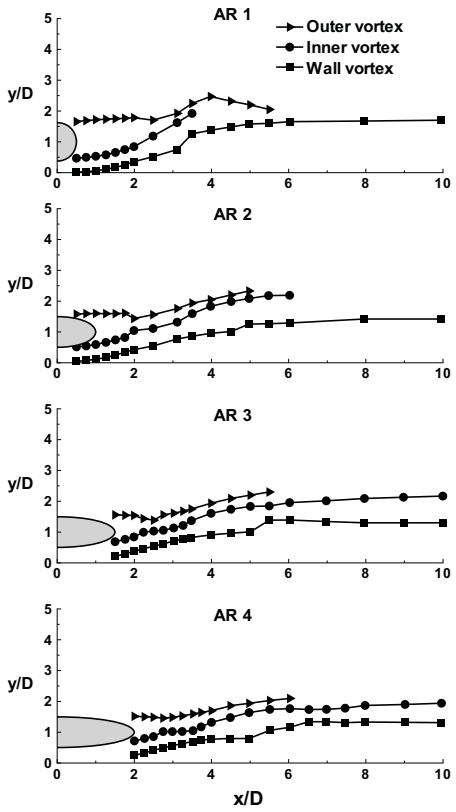

Figure 4: Vortex trajectories of boundary layer and shear layers for AR = 1-4 considering G/D = 0.5.

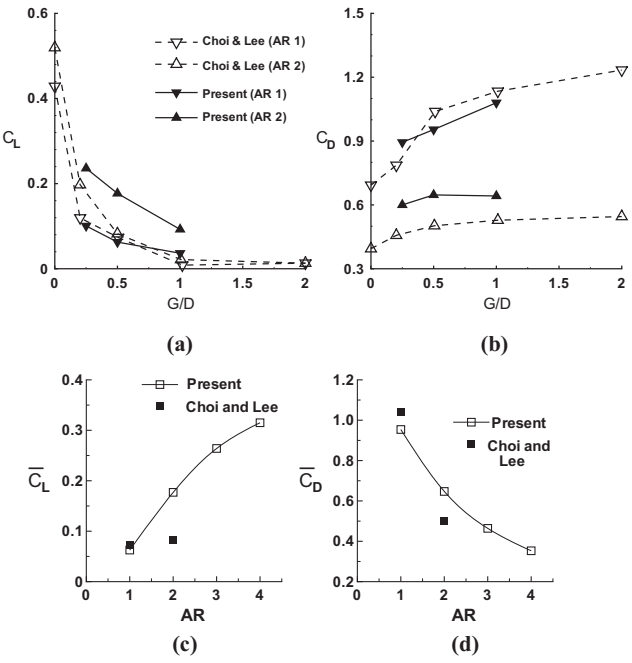

Figure 5: Variation of mean lift and drag coefficients as the gap-ratio (for AR1 and AR2) and shape (for G/D = 0.5) of the cylinder changes.

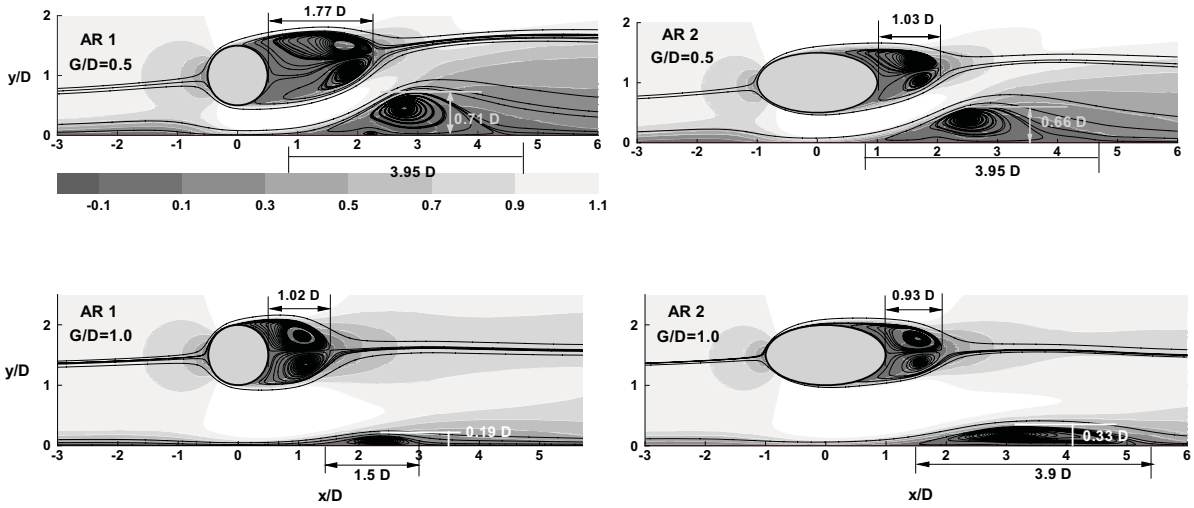

Figure 6: Mean streamwise velocity contours along with streamlines for a circular and an elliptic cylinder (AR2) at different gap-ratios.

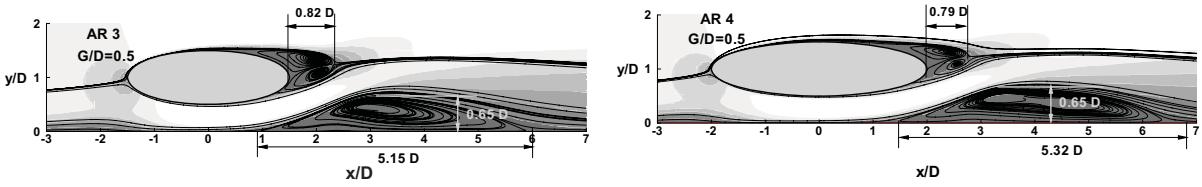

Figure 7: Mean streamwise velocity contours along with streamlines for AR3 and AR4 at a gap of G/D = 0.5.

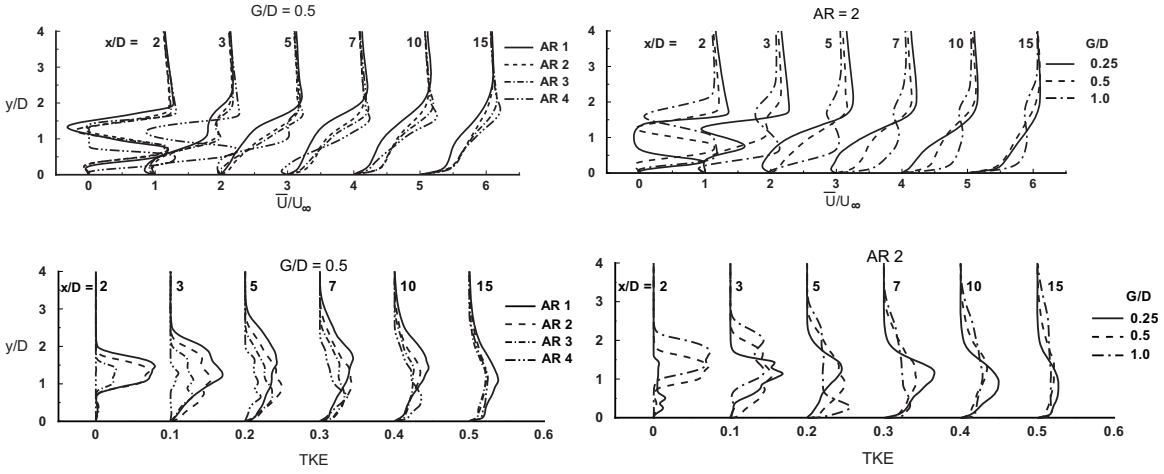

Figure 8: Mean velocity and TKE profiles at x/D = 2, 3, 5, 7, 10 and 15 for different AR and G/D ratios.